Impact of Laser Beam Speckle Structure on Crossed Beam Energy Transfer via Beam Deflections and Ponderomotive Self-Focusing

G. Raj* and S. Hüller
Centre de Physique Théorique (CPHT), Ecole Polytechnique, CNRS, Université Paris-Saclay, 91128 Palaiseau, France
(Received 21 July 2016; published 1 February 2017)

The role of laser speckle structure (hot spots) and its ponderomotive self-focusing (PSF), in crossed beam energy transfer (CBET), of smoothed laser beams is investigated in an inhomogeneous expanding plasma. Numerical simulations using the code HARMONY in two spatial dimensions, demonstrate how self-focusing of laser hot spots in crossed beams can significantly affect the transfer of energy from one beam to the other in addition to the stimulated Brillouin scattering (SBS) process. It is shown that for sufficiently intense laser beams, when the laser hot spots exceed the criterion for self-focusing in a plasma with flow, the angular spread of transmitted light beams increases considerably with the intensity, which arises in particular, in expanding plasma where significant beam deflection is observed. It is shown for the first time that besides SBS, the contribution of speckle structure, PSF, and deflections of the intense hot spots in multiple speckle beams to CBET, therefore matters.

DOI: 10.1103/PhysRevLett.118.055002

Crossed beam energy transfer (CBET) is of prime importance for the modeling and prediction of laser plasma coupling in both the direct-drive [1,2] and the indirect-drive [3–5] inertial confinement fusion (ICF) schemes; it is also the key mechanism for the amplification of short laser pulses by a pump laser pulse [6–8]. In the two schemes of ICF, multiple laser beams cross each other at different angles and directions in a low density plasma on their way to the "hohlraum" wall (indirect drive), and in higher density coronal plasma of the fuel capsule (direct drive). Any two laser beams with wave vectors and frequencies $(\vec{k}_1, \omega_1)$ and $(\vec{k}_2, \omega_2)$, crossing at an angle θ can lead to induced [9,10] or stimulated Brillouin scattering (SBS) of one beam into the other [11–13]. The two beams scatter off ion acoustic waves (IAWs) which are excited due to the beating ponderomotive force. Without loss of generality, allowing also for flow in inhomogeneous plasmas (with velocity $\vec{v}_p$), the SBS is maximum when the beams fulfill the matching conditions: $\vec{k}_s \equiv \vec{k}_1 - \vec{k}_2$ and $\omega_1 - \omega_2 \equiv \omega_s + \vec{k}_s \cdot \vec{v}_p$, where $k_s = 2|k_1| \sin(\theta/2)$ and ω_s are the IAW number and frequency. Thus, the CBET due to SBS redistributes the beam energy beyond the region of beam overlap; in ICF this can seriously degrade laser energy deposition to targets; in schemes designed to amplify shorter pulses, important redistribution due to laser hot spots causes spatially nonhomogeneous energy transfer, as has recently been observed in experiments [8]. All current ICF experiments rely on "smoothed" laser beams which use smoothing techniques like the random phase plates (RPPs) [14,15] to introduce spatial incoherence into the beams. Such beams, on a coarse scale, show a smooth average intensity profile in their cross section, while on a fine laser wavelength (λ_0) scale they have a speckle structure with a statistical distribution of the speckle peak intensity I_{sp} [14–16]. Studying either a single speckle beam or a single RPP beam interacting with inhomogeneous flowing plasma [15–22], and for laser fluxes $I_0\lambda_0^2 \sim 10^{13}$–$10^{15}$ W/cm^2 μm^2, previous studies have shown deflection of laser speckles [23–29], and the interplay between ponderomotive self-focusing (PSF) and SBS [17–22,30]. The current modelings of CBET among multiple RPP beams describe transfer between the overall beams due to SBS [5,31,32], but the role of speckles and their self-focusing in CBET has mostly been disregarded. Although the theory of power transfer between crossed beams has been developed in Ref. [29], the role of speckles and their self-focusing in CBET is missing. In the regime addressed in Refs. [13,33] it was shown that the role of speckles is merely statistical and not particularly pronounced in CBET.

In this Letter, going beyond the statistical aspect of speckles in crossing RPP beams, we demonstrate for the first time how the deflection and the PSF of speckles can significantly affect the CBET due to SBS itself. The usual criterion for ponderomotively self-focusing speckles in a RPP beam is given by $\hat{P} = P/P_c = 0.04\eta(I_{sp}\lambda_0^2/T_e)f^2 n_e/n_c$ with I_{sp} given in 10^{14} W/cm^2, λ_0 in μm, T_e in keV, and with f as the speckle f number; η is a numerical factor of the order of unity, being $\eta = 1.23$ in 2D geometry [34]. Plasma flow, however, in the vicinity where the flow speed equals the sound speed, $v_p \equiv c_s$, modifies the onset of self-focusing [23,24,27], such that the maximum growth of the instability, as a function of the transverse wave number, changes as a function of $\sim 1/(1 - |v_p/c_s|^2)$. Schmitt [24] showed that in the subsonic vicinity of the sonic point, $v_p \leq c_s$, the instability growth is considerably stronger than with no flow at all ($v_p = 0$, as assumed for the above

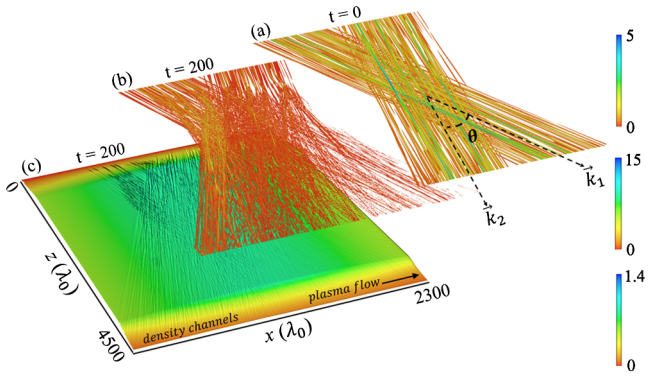

FIG. 1. HARMONY simulations showing interaction of two RPP beams with intensities $I_{01} = I_{02} = 12I_0$, crossing at $\theta = 20°$ at times (a) $t = 0$ and (b) $t = 200(2k_1c_s)^{-1}$; color bars indicate intensities normalized to $12I_0$. (c) Plasma density; normalized to $0.1n_c$ in the color bar.

mentioned criterion). There is no PSF growth for supersonic flow. Consequently, speckles will self-focus at lower intensities than indicated by the above expression for P/P_c. Resonance in a small interval around $v_p \sim c_s$ [23] results in the onset of SBS inside a speckle with energy transfer to the other beam, i.e., speckle-to-beam CBET. Here we study a configuration involving two smoothed beams crossing an angle θ [Fig. 1(a)], in an expanding inhomogeneous plasma. Such a configuration is highly likely to occur in laser entrance holes in indirect-drive ICF experiments, where the plasma is weakly inhomogeneous, both in density and flow [35–40]. Experimental studies with similar configurations have been undertaken recently [8], but also at smaller angles [41,42], or partially at larger angles [43]. Further, there are divergences between results obtained from recent experiments and simulations [44]. While such a study with smoothed beams to this extent has not yet been undertaken, it is of high priority in order to overcome abrupt changes in the angular distribution of the transmitted light in multi-RPP beam configuration experiments. To highlight the distinctness of the present study with respect to those that disregard the role of speckles, we compare results from crossed RPP and "regular" beams (without speckles), but with the same average intensities.

We use the code HARMONY [45,46] in 2D to simulate two s-polarized beams, with $(\vec{k}_1, \omega_1)$ and $(\vec{k}_2, \omega_2)$, that cross at $\theta = 20°$, having the common wave vector component along the positive z direction, while the generated IAWs propagate along with the plasma flow in the x direction. The SBS matching conditions, in this case with $v_p\vec{e}_x$, are satisfied where $v_p(x)/c_s = (\omega_1 - \omega_2 - \sigma\omega_s)/(c_sk_s)$ with σ as the sign of $\omega_1 - \omega_2 - (\vec{k}_1 - \vec{k}_2)\cdot\vec{v}_p$, and where $c_s \equiv [(c_{se}/(1 + k_s^2\lambda_{De}^2)^{1/2} + 3v_i^2]^{-1/2}$ is the IAW velocity, $c_{se} \equiv (ZT_e/m_i)^{1/2}$ with T_e as electron temperature, λ_{De} as Debye length, v_i as the ion thermal velocity, m_i and Z as the ion mass and charge number, respectively. For the profile we have chosen $v_p/c_s = (x - L_x/2 + L_v)/L_v$, with the gradient length $L_v = 200\lambda_0$ as in Ref. [13], SBS matching occurs in the center at $x = L_x/2$ for the case that both beams have equal frequencies, $\omega_1 = \omega_2 = \omega_0$. Hereafter, we denote $I_0\lambda_0^2 \equiv 10^{14}$ W/cm^2 μm^2 as the reference laser flux, and $I_0\lambda_0^2/[T_e(3\text{ keV})]$ as the principal coupling parameter. For the fixed ratio between the average beam intensities considered here, $I_{02}/I_{01} = 1$, the value $I_{02}/I_0 \equiv 1$ in our results corresponds to intensity $I_0 \sim 0.9 \times 10^{15}$ W/cm^2 at $\lambda_0 = 0.35\,\mu$m, for temperatures (fixed) $T_e = 3$ keV and $T_i \ll ZT_e$.

For $a_{01,2} = [I_{01,2}/1.37 \times 10^{18}\text{ W/cm}^2]^{1/2}\lambda_0(\mu\text{m})$ as the normalized field amplitudes, the combined electric fields of the two beams are given by $a_0 = e^{-i\omega_0 t + i\vec{k}_{1\parallel}\cdot\vec{z}}\,[a_{01}e^{i\vec{k}_{1\perp}\cdot\vec{x}} + a_{02}e^{-i\vec{k}_{1\perp}\cdot\vec{x}}] + \text{c.c.}$ [13], with the parallel and transverse wave vector components, $\vec{k}_{1\parallel} = \vec{e}_z|\vec{k}_1|\cos(\theta/2)$ and $\vec{k}_{1\perp} = \vec{e}_x|\vec{k}_1|\sin(\theta/2)$, respectively. The evolution of the wave amplitudes coupled to the plasma density perturbation in HARMONY is described by [46]

$$[c^2\nabla_\perp^2 + 2i\omega_0(\partial_t + v_{gz}\partial_x)]a_0 = \omega_0^2(\delta n/n_c)a_0 \quad (1)$$

with $v_{gz} \equiv (c^2|\vec{k}_1|/\omega_0)\cos(\theta/2)$, and $n_c = m_e\omega_0^2/4\pi e^2$ as the critical density with m_e and e being the electron mass and charge, respectively, $\delta n = (n - n_e)$ is the density perturbation about the equilibrium density n_e described by the hydrodynamic equations

$$\partial_t n + \nabla(n\vec{v}) = 0, \quad (2a)$$

$$[\partial_t + \vec{v}\cdot\nabla]\vec{v} + c_s^2\nabla n/n + \beta\vec{v} = -c_{se}^2[\nabla F_{\text{sbs}} + \nabla F_{\text{psf}}], \quad (2b)$$

where β is the wave-number dependent operator accounting for IAW damping (both collisional and Landau damping) [45,46], $\nabla F_{\text{sbs}} \propto \nabla a_{01}a_{02}^*\exp[2i|\vec{k}_1|x\sin(\theta/2)]$ is the ponderomotive force component acting on the plasma fluid due to the beating between the two waves a_{01} and a_{02} in SBS, whereas $\nabla F_{\text{psf}} \propto \nabla(|a_{01}|^2 + |a_{02}|^2)$ is the component due to ponderomotive self-focusing and forward- SBS in the individual waves.

For all simulations we choose a spatial domain of $L_z \equiv 4500\lambda_0$ and $L_x \equiv 2300\lambda_0$ along the z and x axes, respectively; the plasma density profile is parabolic around the center with $n_e(x) = 0.1n_c\,\exp -[(x - L_x/2)/1615\lambda_0]^2$; we apply linear density ramps over $500\lambda_0$ along z at the laser entry and the rear. Both beams have equal initial intensity $I_{01} = I_{02}$ and a focusing f number [15] of $f = 6$. IAWs are damped with $\beta(k_s) = 0.1\omega_s(k_s)$. CBET due to inhomogeneous flow [13] is present when the effective beam width, $L_{\text{beam}} = D/(2\sin\theta)$ (beam diameter D) is larger than the interaction length

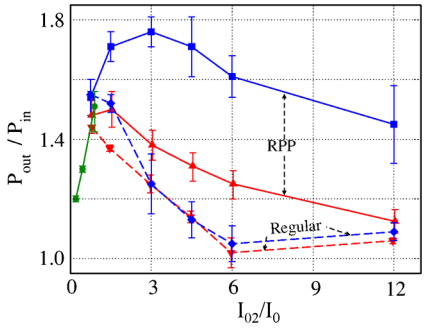

FIG. 2. Power transfer ratio of beam 2, as a function of its input flux I_{02} after exchange with beam 1. Four cases: regular beam case (dashed lines) and RPP case (solid), with (present simulations in blue color and green from Ref. [13]) and without (red) taking into account self-focusing.

$L_{\rm inh} = \pi[\beta(k_s)/\omega_s]L_v/\cos(\theta/2)$, equivalent to $D/L_v > 4\pi(\beta/\omega_s)\sin(\theta/2) \sim 0.2(\theta/20°)(\beta/0.1\omega_s)$ for small θ.

The initial geometry is illustrated in Figure 1(a); Fig. 1(b) shows significant CBET and strong angular spread under the combined effects of beam deflection, SBS, and PSF for the case of high beam intensity $I_{01} = I_{02} = 12I_0$. In Figure 2 we summarize our results from a series of simulations, as a function of I_{02}/I_0, showing clearly that the role of speckles in RPP beams can no longer be disregarded above the reference laser flux, $I_0\lambda_0^2 = 10^{14}$ W/cm^2 μm^2 at $T_e = 3$ keV. To illustrate this we plot power transfer from beam 1 (downwards propagating) to beam 2 as a function of I_{02} $(= I_{01})$. We compare (see Ref. [47]) the power gained by beam 2 for RPPs and regular beam cases in the presence and in the absence of the $\nabla F_{\rm psf}$ force term in the simulations with HARMONY, i.e., by switching on and off this term on the rhs of Eq. (2b).

We obtain the power transfer ratio $(P_{\rm out}/P_{\rm in} \equiv \int_{k_\perp>0}|\hat{a}(k, z = L_z)|^2 dk / \int_{k_\perp>0}|\hat{a}(k, z = 0)|^2 dk)$ from the Fourier transform $\hat{a}(k)$ in $k_\perp$ space of a_0, and use an average of over eight realizations for the RPP cases. While it was shown [33] that for intensities up to $I_{02} \sim 0.75I_0$ speckles play a role only via their abundance in the crossing volume, our results underline the importance of (i) laser speckle structures in CBET and (ii) ponderomotive self-channeling and deflection in inhomogeneous flowing plasma. Figure 2 shows that at lower intensity, for crossed RPPs and regular beams with $I_{02} \le 0.75I_0$, the role of the PSF term is insignificant: the power gained by beam 2 whether with (blue lines) or without the PSF term (in red) converges to the results from Ref. [13] (in green).

Previously, experiments and simulations using crossed RPP beams [11] reported on spectral broadening, in a regime of moderate intensity, low temperature, and collisional absorption. Other similar studies [16–19,19–22,30] either were limited to an isolated laser speckle structure or a single RPP laser beam. Optical mixing effects together with flow were seen in exploding foil experiments [48,49].

Our new results show that as the intensity of the two crossed beams increases, $I_{02} > 0.75I_0$, the power transfer for the RPP case increases, reaches a maximum at $\sim 3I_0$ and then decreases in the presence of PSF (solid blue curve). In contrast to this, without PSF (solid red), but with the $\nabla F_{\rm sbs}$ force only, the transfer decreases almost to unity, $\int_{k_\perp>0}|\hat{a}(k, L_z)|^2 dk \simeq \int_{k_\perp\le 0}|\hat{a}(k, L_z)|^2 dk$, for $I_{02} > I_0$.

Although the above given criteria for PSF indicate that only extreme speckles can have $P_{\rm sp}/P_c > 1$, the presence of flow, giving rise to CBET between beams of equal frequency, considerably changes the PSF in speckles when beams overlap in sonic and subsonic flow regions. Consequently, the light is deflected toward the direction of beam 2, which is a net contribution to CBET for RPP beams (solid curves in Fig. 2) when both contributions of the ponderomotive force, $\nabla F_{\rm sbs}$ and $\nabla F_{\rm psf}$, are taken into account. Hence a portion of beam 1 is effectively deviated along the direction of beam 2 due to PSF till $I_{02}/I_0 \simeq 3$, beyond which the effect tends to diminish for higher intensities. For regular beams (without speckles) the role of PSF and forward SBS is present, but less pronounced. Both results prove the importance of the role of speckles in

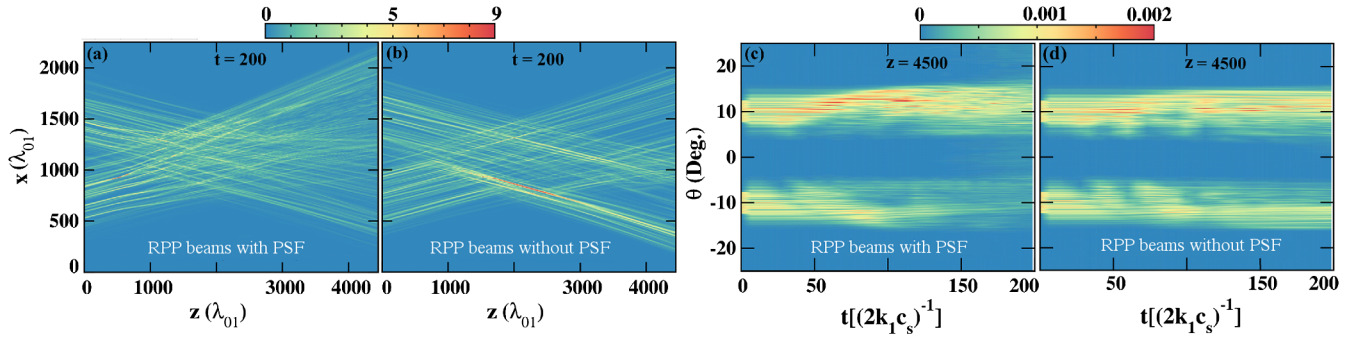

FIG. 3. Subplots (a) and (b): Snapshots from a single realization of the RPP beams showing superposition of intensities of the two crossed beams in space, at $t = 200$ $(2k_1c_s)^{-1}$ ($\sim$11 ps for $\lambda_0 = 0.35$ μm and $T_e = 3$ keV); in (a) both $\nabla F_{\rm sbs}$ and $\nabla F_{\rm psf}$ are retained, while in (b) only the CBET term $\nabla F_{\rm sbs}$. Subplots (c) and (d): Angular spectra of the transmitted light as a function of time, (c) with and (d) without taking in account the $\nabla F_{\rm psf}$ term, computed from of an average over 8 RPP realizations. The color bars show beam intensities normalized to the their average value, i.e., $I_{01} = I_{02} = 6I_0$.

CBET for laser fluxes from $I_{02}\lambda_0^2 > 10^{14}$ W/cm^2 μm^2. Forward SBS in RPP beams can be observed in detail from Fig. 3, for $I_{02} = 6I_0$: Fig. 3(a) shows that in the presence of PSF, the two crossed RPP beams undergo significant deflection (relative to their initial propagation direction, see Fig. 1) in an angular aperture broader than initially, while this effect is much less pronounced without the $\nabla F_{\rm psf}$ force, see Fig. 3(b). Also, Fig. 3(a) illustrates features of plasma induced smoothing [34] and "dancing beamlets" [30] at the rear of the simulation box, due to the action of both terms, $\nabla F_{\rm psf}$ and $\nabla F_{\rm sbs}$. In contrast to this, two crossed "regular" beams are redirected considerably toward their common axis (see Ref. [47]).

To illustrate the effect of deflection and angular broadening seen for crossed RPP beams in Figs. 3(a–b), we plot the temporal evolution of angular spectrum of the transmitted light (detected at the simulation window right edge), respectively, in Figs. 3(c) and 3(d). The light signals appearing in the upper right corner of the simulation box between time $t = 150$ and 200 in Fig. 3(c), in the presence of PSF, show components up to large (i.e. $\approx 25°$) angles in beam 2. For this case ($I_{02} = 6I_0$, see also Ref. [50]), the mean angle and the standard deviations evolve from $10° \pm 3.5°$ at $t = 0$ to $11° \pm 7°$ at $t = 200$, while in the absence of the $\nabla F_{\rm psf}$ term, Fig. 3(d), beam 2 does not undergo strong deflection, but shows an asymmetric angular spread around $11.5°(+5°/-4°)$, at $t = 200$. Similarly, beam 1, as seen in Fig. 3(c), undergoes enhanced angular broadening around $-10° \pm 5.5°$, while for the case without PSF, see Fig. 3(d), beam 1 shows asymmetry around $-12°(+5°/-4°)$ due to depletion.

The observed broadening in our simulations of the overall angular spectrum for the case with both $\nabla F_{\rm psf}$ and $\nabla F_{\rm sbs}$ is systematically worked out in Fig. 4: in a stage where CBET processes have mostly settled down, $t = 200$, the comparison between the angular distribution of transmitted light of the two crossed beams is shown for the RPP beam cases in the presence [Fig. 4(a)] and in the absence [Fig. 4(b)] of $\nabla F_{\rm psf}$ (see also Ref. [47] for results from "regular" beams). Clearly, RPP beams exhibit, due to their speckle structure, an increasing angular spread of transmitted light with increasing intensity, more pronounced with the $\nabla F_{\rm psf}$ term, while for regular beams [47] mainly a strong central beam structure close to $\theta \sim 0$ appears incrementally, depleting beam 1 around $\theta = 10°$. In strong contrast to regular beams [47], for the RPP case two distinguished beams can always be identified, with only weak beam components around $\theta \sim 0$.

The decrease of the transfer after a maximum, seen in Fig. 2 for $I_{02}/I_0 > 3$ with PSF (and $I_{02}/I_0 > 1$ without), is correlated with both (i) the increment of angular spread, associated with enhanced spatial and temporal incoherence, of each beam with increasing beam power, and (ii) the onset of nonlinearities in the IAW perturbations. We observe that both self-channeling speckles, as well as the IAWs induced

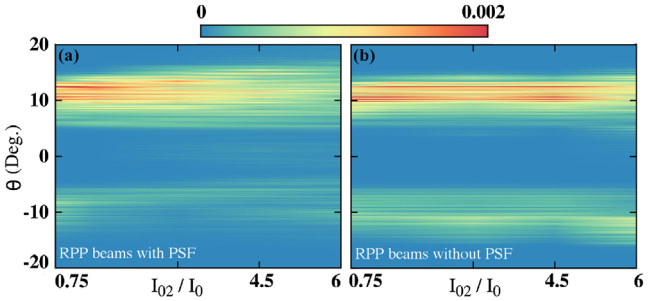

FIG. 4. Contour plots of angular spectra of the transmitted light, as a function of the incident intensity I_{02}/I_0 for $I_{01} = I_{02}$, taken at $x/\lambda_0 = 4000$ and $t = 200$, for RPP beams (ensemble average): in (a) the $\nabla F_{\rm psf}$ term in simulations is omitted, in (b) the term is retained. Note: Color bar values are normalized to the total power ($\propto I_{02}$) of beam 2.

by SBS of CBET, provoke density perturbations that tend to steepen and evolve nonlinearly, resulting in deflection and a broader angular spread of the beams [26,28,51]. In Fig. 5 we show the wave number spectra of IAW perturbations, taken at a central cut $z/\lambda_0 = 1800$. Besides the CBET wave number at $2|\vec{k}_1|\sin(\theta/2)$, components related to the speckle imprint ($\simeq 0.08k_1$) and harmonics arise only due to speckle-to-beam transfer (not present for regular beams) in the presence of PSF. Also, due to the light scattering off these components and the partial angular redirection of the beams, the net transfer to beam 2 decreases because the coupling of the fundamental IAW from CBET is weakened.

Density perturbations driven by crossed RPP beams lead to stochastic ion heating [52] on the hydrodynamics scale over 0.1 ns. Its effect on IAW damping may play a minor role for CBET in inhomogeneous flow. While ion trapping effects were observed to counteract CBET for weakly damped IAWs [38,39] or in homogeneous plasmas [53],

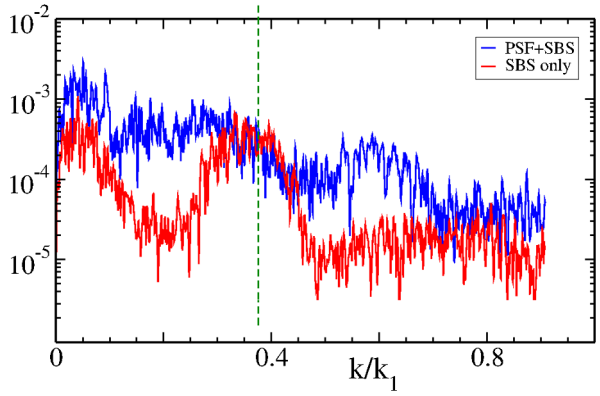

FIG. 5. Fourier transform of ion density perturbations in x at a cut $z/\lambda_0 = 1800$ in the crossing region of RPP beams as a function of the wave number $k_\perp/|\vec{k}_1|$, taken at $t = 200$. Blue (red) curve: with (without) the $\nabla F_{\rm psf}$ term. Dashed green line: $k_\perp/|\vec{k}_1| \equiv 2\sin(\theta/2) \simeq 0.34$.

this should have small impact at higher damping, and because of inhomogeneous flow advection.

Spatiotemporal smoothing with sufficient band width, such as smoothing by spectral dispersion (SSD) or induced spatial incoherence (ISI), may be able to control CBET and the onset of self-focusing by introducing finite speckle life time and larger beam aperture. SSD has been used in experiments at NIF and at the Omega laser facility [1,40], while the onset of CBET remains a pending problem with the available band width.

In conclusion we have demonstrated that laser beam speckle structure plays an important role for crossed beam energy transfer when self-focusing of speckles occurs, an aspect that has been neglected in previous studies on CBET. For plasmas with inhomogeneous profiles, where CBET occurs around sonic flow, the onset of self-focusing speckles is enhanced. The latter leads to considerable beam deflection and enhanced angular width of the transmitted laser beams. Angular broadening can be attributed to plasma-induced smoothing and scattering off nonlinear density perturbations [47]. Beam deflection and broadening are important issues for laser energy deposition in ICF and they will have strong impact on schemes designed to amplify short laser pulses by longer pulses via CBET.

We thank W. Rozmus and D. Pesme for helpful discussions. This work has been partially supported by Agence Nationale de la Recherche (France), project title "Ilphygerie" No. ANR-12-BS04-0006.

*gaurav.raj@polytechnique.edu

[1] I. V. Igumenshchev *et al.*, Phys. Plasmas **19**, 056314 (2012).
[2] J. F. Myatt *et al.*, Phys. Plasmas **21**, 055501 (2014).
[3] P. Michel *et al.*, Phys. Plasmas **16**, 042702 (2009).
[4] J. D. Moody *et al.*, Nat. Phys. **8**, 344 (2012).
[5] P. Michel *et al.*, Phys. Rev. Lett. **102**, 025004 (2009).
[6] L. Lancia, J.-R. Marquès, M. Nakatsutsumi, C. Riconda, S. Weber, S. Hüller, A. Mančić, P. Antici, V. T. Tikhonchuk, A. Héron, P. Audebert, and J. Fuchs, Phys. Rev. Lett. **104**, 025001 (2010).
[7] E. Guillaume *et al.*, High Power Laser Sci. Eng. **2**, e33 (2014).
[8] C. Neuville, C. Baccou, A. Debayle, P.-E. Masson-Laborde, S. Hüller, M. Casanova, D. Marion, P. Loiseau, K. Glize, C. Labaune, and S. Depierreux, Phys. Rev. Lett. **117**, 145001 (2016).
[9] W. L. Kruer, S. C. Wilks, B. B. Afeyan, and R. K. Kirkwood, Phys. Plasmas **3**, 382 (1996).
[10] R. K. Kirkwood, B. B. Afeyan, W. L. Kruer, B. J. MacGowan, J. D. Moody, D. S. Montgomery, D. M. Pennington, T. L. Weiland, and S. C. Wilks, Phys. Rev. Lett. **76**, 2065 (1996).
[11] C. Labaune, H. A. Baldis, E. Schifano, B. S. Bauer, A. Maximov, I. Ourdev, W. Rozmus, and D. Pesme, Phys. Rev. Lett. **85**, 1658 (2000).
[12] C. Labaune, H. A. Baldis, B. Cohen, W. Rozmus, S. Depierreux, E. Schifano, B. S. Bauer, and A. Michard, Phys. Plasmas **6**, 2048 (1999).
[13] A. Colaïtis, S. Hüller, D. Pesme, G. Duchateau, and V. T. Tikhonchuk, Phys. Plasmas **23**, 032118 (2016).
[14] Y. Kato and K. Mima, Appl. Phys. B **29**, 186 (1982).
[15] H. A. Rose and D. F. DuBois, Phys. Fluids B **5**, 3337 (1993).
[16] H. A. Rose and D. F. DuBois, Phys. Fluids B **5**, 590 (1993).
[17] M. R. Amin, C. E. Capjack, P. Frycz, W. Rozmus, and V. T. Tikhonchuk, Phys. Fluids B **5**, 3748 (1993).
[18] S. Hüller, P. Mounaix, and D. Pesme, Phys. Scr. **T63**, 151 (1996).
[19] V. T. Tikhonchuk, S. Hüller, and P. Mounaix, Phys. Plasmas **4**, 4369 (1997).
[20] P. E. Masson-Laborde, S. Hüller, D. Pesme, C. Labaune, S. Depierreux, P. Loiseau, and H. Bandulet, Phys. Plasmas **21**, 032703 (2014).
[21] H. A. Rose, Phys. Plasmas **2**, 2216 (1995).
[22] R. L. Berger, B. F. Lasinski, A. B. Langdon, T. B. Kaiser, B. B. Afeyan, B. I. Cohen, C. H. Still, and E. A. Williams, Phys. Rev. Lett. **75**, 1078 (1995).
[23] R. W. Short, R. Bingham, and E. A. Williams, Phys. Fluids **25**, 2302 (1982).
[24] A. J. Schmitt, Phys. Fluids B **1**, 1287 (1989).
[25] P. E. Young, C. H. Still, D. E. Hinkel, W. L. Kruer, E. A. Williams, R. L. Berger, and K. G. Estabrook, Phys. Rev. Lett. **81**, 1425 (1998).
[26] D. S. Montgomery, R. P. Johnson, H. A. Rose, J. A. Cobble, and J. C. Fernández, Phys. Rev. Lett. **84**, 678 (2000).
[27] H. A. Rose, Phys. Plasmas **3**, 1709 (1996).
[28] D. E. Hinkel, E. A. Williams, and C. H. Still, Phys. Rev. Lett. **77**, 1298 (1996).
[29] H. A. Rose and S. Ghosal, Phys. Plasmas **5**, 1461 (1998).
[30] A. J. Schmitt and B. B. Afeyan, Phys. Plasmas **5**, 503 (1998).
[31] J. A. F. Hittinger, M. R. Dorr, R. L. Berger, and E. A. Williams, J. Comput. Phys. **209**, 695 (2005).
[32] P. Michel *et al.*, Phys. Plasmas **17**, 056305 (2010).
[33] A. Colaitis, S. Hüller, V. T. Tikhonchuk, D. Pesme, G. Duchateau, and A. Porzio, J. Phys. Conf. Ser. **717**, 012096 (2016).
[34] A. V. Maximov, I. G. Ourdev, D. Pesme, W. Rozmus, V. T. Tikhonchuk, and C. E. Capjack, Phys. Plasmas **8**, 1319 (2001).
[35] D. E. Hinkel, M. B. Schneider, E. A. Williams, A. B. Langdon, L. J. Suter, and P. T. Springer, in *Inertial Fusion Sciences and Applications 2003*, edited by J. Meyer-ter-Vehn, B. A. Hammel, D. D. Meyerhofer, and H. Azechi (Elsevier, Amsterdam, 2004), pp. 242–246.
[36] E. A. Williams, D. E. Hinkel, and J. A. Hittinger, in *Inertial Fusion Sciences and Applications 2003*, edited by J. Meyer-ter-Vehn, B. A. Hammel, D. D. Meyerhofer, and H. Azechi (Elsevier, Amsterdam, 2004), pp. 252–255.
[37] D. E. Hinkel, D. A. Callahan, A. B. Langdon, S. H. Langer, C. H. Still, and E. A. Williams, Phys. Plasmas **15**, 056314 (2008).
[38] R. K. Kirkwood, J. D. Moody, A. B. Langdon, B. I. Cohen, E. A. Williams, M. R. Dorr, J. A. Hittinger, R. Berger, P. E. Young, L. J. Suter, L. Divol, S. H. Glenzer, O. L. Landen, and W. Seka, Phys. Rev. Lett. **89**, 215003 (2002).
[39] R. K. Kirkwood, E. A. Williams, B. I. Cohen, L. Divol, M. R. Dorr, J. A. Hittinger, A. B. Langdon, C. Niemann, J. Moody, L. J. Suter, and O. L. Landen, Phys. Plasmas **12**, 112701 (2005).

[40] R. K. Kirkwood *et al.*, Phys. Plasmas **18**, 056311 (2011).
[41] R. K. Kirkwood, B. J. MacGowan, D. S. Montgomery, B. B. Afeyan, W. L. Kruer, D. M. Pennington, S. C. Wilks, J. D. Moody, K. Wharton, C. A. Back, K. G. Estabrook, S. H. Glenzer, M. A. Blain, R. L. Berger, D. E. Hinkel, B. F. Lasinski, E. A. Williams, D. Munro, B. H. Wilde, and C. Rousseaux, Phys. Plasmas **4**, 1800 (1997).
[42] D. S. Montgomery, B. B. Afeyan, J. A. Cobble, J. C. Fernández, M. D. Wilke, S. H. Glenzer, R. K. Kirkwood, B. J. MacGowan, J. D. Moody, E. L. Lindman, D. H. Munro, B. H. Wilde, H. A. Rose, D. F. Dubois, B. Bezzerides, and H. X. Vu, Phys. Plasmas **5**, 1973 (1998).
[43] K. B. Wharton, R. K. Kirkwood, S. H. Glenzer, K. G. Estabrook, B. B. Afeyan, B. I. Cohen, J. D. Moody, B. J. MacGowan, and C. Joshi, Phys. Plasmas **6**, 2144 (1999).
[44] A. Pak, E. L. Dewald, O. L. Landen, J. Milovich, D. J. Strozzi, L. F. Berzak Hopkins, D. K. Bradley, L. Divol, D. D. Ho, A. J. MacKinnon, N. B. Meezan, P. Michel, J. D. Moody, A. S. Moore, M. B. Schneider, R. P. J. Town, W. W. Hsing, and M. J. Edwards, Phys. Plasmas **22**, 122701 (2015).
[45] S. Hüller, P. E. Masson-Laborde, D. Pesme, M. Casanova, F. Detering, and A. Maximov, Phys. Plasmas **13**, 022703 (2006).
[46] D. Pesme, S. Hüller, J. Myatt, C. Riconda, A. Maximov, V. T. Tikhonchuk, C. Labaune, J. Fuchs, S. Depierreux, and H. A. Baldis, Plasma Phys. Controlled Fusion **44**, B53 (2002).
[47] See Supplemental Material at http://link.aps.org/supplemental/10.1103/PhysRevLett.118.055002 for further details regarding the comparison between RPP and regular beams.
[48] B. B. Afeyan, C. Geddes, D. S. Montgomery, R. K. Kirkwood, P. Bellomo, K. Estabrook, C. Decker, D. Meyerhofer, S. Regan, W. Seka, R. P. J. Town, and A. J. Schmitt, in *Inertial Fusion Sciences and Applications 99*, edited by W. H. C. Labaune and K. Tanaka (Elsevier, Amsterdam, 2000), pp. 331–335.
[49] B. B. Afeyan, M. Mandirian, K. Won, D. S. Montgomery, J. Hammer, R. K. Kirkwood, and A. J. Schmitt, in *Inertial Fusion Sciences and Applications 2003*, edited by J. Meyerter-Vehn, B. A. Hammel, D. D. Meyerhofer, and H. Azechi (Elsevier, Amsterdam, 2004) pp. 264–267.
[50] For the case of RPP beams with $I_{02} = I_{01} = 0.75I_0$, the mean angle and the standard deviations at $t = 200$ are $\sim 11° \pm 4°$ for beam 2, and $\sim -9.0° \pm 4°$ for beam 1.
[51] J. Myatt, D. Pesme, S. Hüller, A. Maximov, W. Rozmus, and C. E. Capjack, Phys. Rev. Lett. **87**, 255003 (2001).
[52] P. Michel, W. Rozmus, E. A. Williams, L. Divol, R. L. Berger, R. P. J. Town, S. H. Glenzer, and D. A. Callahan, Phys. Rev. Lett. **109**, 195004 (2012).
[53] D. J. Y. Marion, A. Debayle, P.-E. Masson-Laborde, P. Loiseau, and M. Casanova, Phys. Plasmas **23**, 052705 (2016).